Optimal Adaptation of 3D Beamformers in UAV Networks

Kasun Prabhath
CISL, ECE Department
University of New Mexico
Albuquerque, NM, USA
Email: prabhathgwk@unm.edu

Sudharman K. Jayaweera
CISL, ECE Department
University of New Mexico
Albuquerque, NM, USA
Email: jayaweera@unm.edu

***Abstract*—The optimal beamformer weight update timing is derived for 3D beamforming between Unmanned Aerial Vehicles (UAVs). The use of optimal update period (Δt^*) ensures that beamforming gain (G_{tx}) drops below a required threshold least frequently. When the exact flight path of the UAV receiver (UAV-RX) is available, the proposed optimization problem calculates optimal Δt^* exactly. It is shown that when the antenna aperture is fixed, the optimal Δt^* monotonically decreases as the operating frequency increases. As a result, the beamformer needs to be updated more often when using higher frequencies. However, it is shown that the fractional overhead relative to the large bandwidths available in mmWave spectrum can still be lower, justifying the use of mmWave frequencies in UAV-to-UAV communications. When exact flight path knowledge is not available, the proposed algorithm incorporates UAV-RX location predictions to update the beamforming weights in a timely manner. The proposed method was simulated in a UAV communication system and the performance of the system is analyzed in terms of the UAV-RX location prediction error. The findings indicate that when there are location prediction errors, incorporating a gain margin to the minimum gain threshold further enhances the algorithm's performance by approximately 10-20%.**

***Index Terms*—UAV communication, 3D beamforming, mmwave**

I. Introduction

Millimeter wave (mmWave) communications is expected to meet the capacity and connectivity requirements of 6G. However, certain aspects of high frequency communication systems make it challenging to establish fast and reliable connections. For example, compared to lower frequency antennas, mmWave massive antenna arrays can produce highly directional and much narrower beams. It can be challenging to align such narrow beams in a communication link even when nodes are stationary [1].

With the advent of new applications, the use of drones is becoming more widespread. For example, Unmanned Aerial Vehicles (UAVs) have found many applications in cellular UAV communication, mobile communications, surveillance, aerial photography, search & rescue missions and disaster relief [2]. In many of these emerging applications, direct communication between UAVs are expected to be reliable and fast [3]. Similar to device-to-device (D2D) terrestrial communications, cellular UAV-to-UAV (U2U) communications may also bring benefits in terms of spectral and energy efficiencies and reduced backhaul operations [4].

Recent research on 3D beamforming provides promising methods to improve the efficiency of wireless communication systems in several aspects [1]. However, in U2U mmWave communications, the high-speed mobility may make it increasingly difficult to align the transmitter and receiver beams. Indeed, even in a UAV-to-ground communication system, there are many difficulties to overcome to maintain fast and reliable communications [5]. Still, UAV-to-ground communication systems have benefited from the use of recently developed 3D beamforming technologies [6]. For example, the authors of [7] proposed a method to update beamforming weights at the receiver based on the received signal. In this method, the receiver tracks the Angle of Arrival (AOA) of the received signal to update its beamforming weights.

The high mobility of the UAVs may expect to require more frequent changes in the beams depending on the relative locations of the transmitter and the receiver. Even a slight deviation of the beam alignment can cause significant loss in the communication link. In this paper we investigate this problem in U2U communications that employ 3D beamforming. We first derive the optimal beamforming weights update time period assuming the knowledge of full trajectory of the UAV-RX (UAV receiver). Next, we propose a method to update the beamforming weights by predicting the location of the UAV-RX for a certain time period ahead. The effectiveness of the proposed algorithm and its behaviour in systems operating in low and high frequencies and the dependence of beamforming gain on the prediction error is also investigated.

The rest of the paper is organized as follows: Section II presents the system model for U2U communications, Section III derives the optimal 3D beamforming weights update timing, Section IV shows the simulation results based on trajectories in an example UAV network and, finally, Section V concludes the paper.

II. The system model for U2U communications

We consider a typical UAV network in which U2U communications is between a UAV-TX (UAV transmitter) and a UAV-RX as shown in Fig. 1. The UAV-TX is equipped with M_{tx} number of antenna elements where $M_{tx} = M_{tx}^x M_{tx}^y$ and

UAV-RX is equipped with M_{rx} number of receiver antenna elements where $M_{rx} = M_{rx}^x M_{rx}^y$. The number of elements in the UAV-TX antenna's horizontal and vertical directions are assumed to be M_{tx}^x and M_{tx}^y, respectively. Similarly, M_{rx}^x and M_{rx}^y, are the number of elements in the UAV-RX's array in each direction.

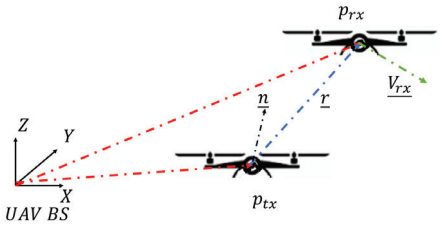

Fig. 1. A UAV-to-UAV communication system

The received complex baseband signal at the UAV-RX $Y \in \mathbb{C}^{M_{rx}\times 1}$ can be expressed as $Y = \sqrt{p}HX + Z$ where $H \in \mathbb{C}^{M_{rx}\times M_{tx}}$ is the LOS channel coefficients matrix from UAV-TX to the UAV-RX, $X \in \mathbb{C}$ is the transmit signal vector, p is the transmit symbol power and $Z \in \mathbb{C}^{M_{rx}\times 1}$ is the receiver noise vector at the UAV-RX. The transmit signal vector X can be expressed as $X = \underline{w}_t x$ where $\underline{w}_t \in \mathbb{C}^{M_{tx}\times 1}$ is the transmit beamformer weight vector and $x \in \mathbb{C}$ is the transmit symbol. The channel coefficient matrix can be expressed as $H = \alpha \underline{a}_{rx}\underline{a}_{tx}^H$ where $\alpha \in \mathbb{R}_{\geq 0}$ is the LOS path gain from the UAV-TX to the UAV-RX [8], $\underline{a}_{tx} \in \mathbb{C}^{M_{tx}\times 1}$ is the array response vector at the UAV-TX antenna based on the UAV-RX location and $\underline{a}_{rx} \in \mathbb{C}^{M_{rx}\times 1}$ is the array response vector at the UAV-RX corresponding to the received signal from the UAV-TX. The LOS path loss α can be represented as [8],

$$\alpha = \sqrt{\frac{g_t g_r \lambda^2}{(4\pi r)^2} f^{tx}(\theta^{rx}, \varphi^{rx}) f^{rx}(\theta^{tx}, \varphi^{tx})}$$

where g_t and g_r are the UAV-TX and UAV-RX antenna element gains, θ^{rx} and φ^{rx} are the elevation and azimuth angles of the UAV-RX with respect to the UAV-TX antenna orientation, θ^{tx} and φ^{tx} are the elevation and azimuth angles of the UAV-TX with respect to the UAV-RX antenna orientation, $f^{rx}(\theta^{tx}, \varphi^{tx})$ is the normalized beam pattern of the UAV-RX antenna elements, $f^{tx}(\theta^{rx}, \varphi^{rx})$ is the normalized beam pattern of the UAV-TX antenna elements and r is the distance between the UAV-TX and UAV-RX. Using these definitions, the received signal vector Y can be written as

$$Y = \sqrt{\frac{p g_t g_r \lambda^2}{(4\pi r)^2} f^{tx}(\theta^{rx}, \varphi^{rx}) f^{rx}(\theta^{tx}, \varphi^{tx})}\, \underline{a}_{rx}\underline{a}_{tx}^H X + Z$$

so that the received signal power can be expressed as

$$P_y = \frac{p g_t g_r \lambda^2}{(4\pi r)^2} f^{tx}(\theta^{rx}, \varphi^{rx}) f^{rx}(\theta^{tx}, \varphi^{tx}) \left\| \underline{w}_r^H \underline{a}_{rx}\underline{a}_{tx}^H X \right\|^2 + P_z$$

where $\underline{w}_r \in \mathbb{C}^{M_{rx}\times 1}$ is the receiver beamforming weight vector and P_z is the received signal noise power. The transmitter beamforming gain G_{tx} can be defined as

$$G_{tx} = \left\| \frac{1}{M_{tx}^x M_{tx}^y} f^{tx}(\theta^{rx}, \varphi^{rx})^{1/2} \underline{a}_{tx}^H \underline{w}_t \right\|^2 .$$

Note that, while radiation pattern of antenna elements depends on the particular structure of the antenna and thus is fixed, it is possible to control G_{tx} electrically using the beamforming weights, $\underline{w}_t$, at the transmitter.

For later use, we introduce the notation $e(\varphi, \theta, M^x, M^y, d^x, d^y) = \underline{p}^y \otimes \underline{p}^x$ where $\underline{p}^y = [1, e^{q_y}, ..., e^{(M^y-1)q_y}]^T$, $q_y = j2\pi d^y \sin\theta \sin\varphi/\lambda$, $\underline{p}^x = [1, e^{q_x}, ..., e^{(M^x-1)q_x}]^T$, $q_x = j2\pi d^x \sin\theta\cos\varphi/\lambda$ and d^x and d^y are the element spacing along the vertical and horizontal directions of the transmit/receive antenna arrays, respectively.

III. 3D Beamforming Weight Vector Update Timing

By supporting a large number of elements in a smaller aperture, mmWave antennas can produce highly directional narrow beams. However, even a slight misalignment in such narrow beams could result in significant signal loss at the UAV-RX. As a result, due to the mobility of both UAV-RX and UAV-TX, it is important to maintain the alignment of both beams in order to ensure a reliable connection. To accomplish this, beamforming weights have to be updated sufficiently fast in accordance with relative movement of the two UAVs. Timely adaptation of the beamforming weight $\underline{w}_t$ allows maintaining the required beamforming gain G_{tx} enabling the received signal power to remain above a minimum desired threshold. For timely update of transmit beamforming weights, this paper proposes an algorithm based on estimated positions of UAV-TX and UAV-RX.

A. Optimal 3D beamforming weight vector update timing

Without loss of generality, let us consider the relative motion of a UAV-RX with respect to the UAV-TX as illustrated in Fig. 1. Let X_t^{rx}, φ_t^{rx} and θ_t^{rx} be the location vector, azimuth angle and elevation angle of the UAV-RX with respect to the UAV-TX at time t, based on a coordinate system where the Z axis is perpendicular to the UAV-TX's planner antenna array. Similarly, let $\varphi_{t+\Delta t}^{rx}$ and $\theta_{t+\Delta t}^{rx}$ be the corresponding angles of the UAV-RX at time $t + \Delta t$. The relationship between $(\varphi_t^{rx}, \theta_t^{rx})$ and $(\varphi_{t+\Delta t}^{rx}, \theta_{t+\Delta t}^{rx})$ can be expressed as $\varphi_{t+\Delta t}^{rx} = \varphi_t^{rx} + \Delta\varphi_t^{rx}$ and $\theta_{t+\Delta t}^{rx} = \theta_t^{rx} + \Delta\theta_t^{rx}$ where $\Delta\varphi_t^{rx}$ and $\Delta\theta_t^{rx}$ represent the variation of φ^{rx} and θ^{rx} from time t to $t+\Delta t$, respectively, and are give by $\Delta\varphi_t^{rx} = \int_t^{t+\Delta t} \dot{\varphi}^{rx}(\tau) d\tau$ and $\Delta\theta_t^{rx} = \int_t^{t+\Delta t} \dot{\theta}^{rx}(\tau) d\tau$. It can be seen that in the absence of noise, the optimal transmit beamforming weight vector based on UAV-RX location, at time t_0 are given by $\underline{w}_{t_0} = e(\theta_{t_0}^{rx}, \varphi_{t_0}^{rx}, M_{rx}^x, M_{rx}^y, d^x, d^y)$. The transmit antenna steering vector corresponding to time $t + \Delta t$ can be given as [9]

$$\begin{aligned} \underline{a}_{tx}(t+\Delta t) &= e(\varphi_{t+\Delta t}^{rx}, \theta_{t+\Delta t}^{rx}, M_{rx}^x, M_{rx}^y, d^x, d^y) \\ &= e(\varphi_t^{rx} + \Delta\varphi_t^{rx}, \theta_t^{rx} + \Delta\theta_t^{rx}, M_{rx}^x, M_{rx}^y, d^x, d^y). \end{aligned}$$

Therefore, the transmitter beamforming gain at time $t + \Delta t$ can be written as

$$G_{tx} = \left\| f^{tx}(\theta_t^{rx} + \Delta\theta_t^{rx}, \varphi_t^{rx} + \Delta\varphi_t^{rx}) \right\| \left\| \frac{\sin(M_{tx}^x \Phi_x/2)}{M_{tx}^x \sin(\Phi_x/2)} \frac{\sin(M_{tx}^y \Phi_y/2)}{M_{tx}^y \sin(\Phi_y/2)} \right\|^2 \quad (1)$$

where

$$\Phi_x = \frac{2\pi d^x}{\lambda} \sin(\theta_t^{rx} + \Delta\theta_t^{rx}) \cos(\varphi_t^{rx} + \Delta\varphi_t^{rx}) - \frac{2\pi d^x}{\lambda} \sin(\theta_{t_0}^{rx}) \cos(\varphi_{t_0}^{rx})$$

and

$$\Phi_y = \frac{2\pi d^y}{\lambda} \sin(\theta_t^{rx} + \Delta\theta_t^{rx}) \sin(\varphi_t^{rx} + \Delta\varphi_t^{rx}) - \frac{2\pi d^y}{\lambda} \sin(\theta_{t_0}^{rx}) \sin(\varphi_{t_0}^{rx}).$$

Frequent update of beamforming weights requires frequent transmission of training bits [10]. Therefore maximization of Δt reduces the training overhead. However, it may also reduce the beamforming gain as seen from (1). Based on the relative angular velocities $\dot{\theta}_t^{rx}$ and $\dot{\varphi}_t^{rx}$ of UAV-RX with respect to the UAV-TX, the optimal Δt, denoted as Δt^*, to maintain a minimum required beamforming gain $G_{tx,\min}$ can be expressed as

$$\Delta t^* = \max_{\Delta t} \quad \Delta t \quad \text{s.t.} \quad G_{tx}(X_{t+\Delta t}^{rx}) \geq G_{tx,\min} \quad . \quad (2)$$

Due to the form of (1), in general, Δt^* can not be expressed in closed form but can only be determined numerically. Moreover, calculation of Δt^* requires the knowledge of the UAV-RX trajectory from time t to $t + \Delta t$, requiring the complete knowledge or estimation of the relative flight paths of the UAVs.

As a special case, let us assume that the UAV-RX is moving only in the elevation plane (i.e $\dot{\varphi}_t^{rx} = 0$). In addition, we will assume that $\varphi_t^{rx} = 0$ and constant relative angular velocity of UAV-RX with respect to UAV-TX is ω_{rx}. Let Δt_{el}^* be the Δt^* corresponds to this scenario. In this case, the Δt_{el} to maintain a required minimum transmit beamforming gain of $G_{tx,\min}$ can be expressed in closed form as,

$$\Delta t_{el}^* = \frac{\sin^{-1}\left(\frac{sinc^{-1}(\sqrt{G_{tx,\min}})}{M_{tx}^x(\pi \frac{d^x}{\lambda})} + \sin(\theta_t^{rx}) \right) - \theta_t^{rx}}{\omega_{rx}}.$$

However, in general, the relative UAV movement may not be confined to the elevation plane in a real U2U communication system. When that is the case, even if the complete relative flight path of the UAV-RX is available, calculating Δt^* numerically can still be computationally demanding.

B. Beamforming weights update algorithm with location predictions

UAV flight path may either be predefined or varied with time according to the current status of the network. In light of this, the UAV-TX must determine the optimal beamforming update period while tracking the UAV-RX flight path. In recent research, there are several promising methods developed for UAV-flight path prediction, including, for example, Kalman filter [11] and machine learning [12], [13]. Past flight path information may be utilized by the Algorithm (in step 1) to predict the relative flight path of the UAV-RX depending on the prediction method used. The accuracy of UAV-flight path prediction can be characterized by the prediction error variance.

In the following, we propose an algorithm to update the beamforming vector at optimal update times by using UAV-RX location predictions. Based on the present estimate of UAV-RX location, the proposed algorithm calculates Δt^* at current time instant t as shown in Fig. 2. If UAV-RX is moving away from the UAV-TX signal transmit range, for example, Δt^* will keep reducing with time. Once Δt^* reaches the minimum prediction error threshold, the proposed algorithm will update $\underline{w}_t$.

The estimated location of UAV-RX is perturbed by measurement noise and prediction error [13]. Let us denote $\hat{X}_{t|t}^{rx}$ as the estimated location of the UAV-RX w.r.t. UAV-TX based on measurement and other information available at time t. The relationship between predicted and true UAV-RX location with respect to the UAV-TX can be represented as

$$\hat{X}_{t+\Delta t|t}^{rx} = X_{t+\Delta t}^{rx} + N_{\Delta t}$$

where $\hat{X}_{t+\Delta t|t}^{rx}$ is the predicted location of the UAV-RX w.r.t. UAV-TX based on $\hat{X}_{t|t}^{rx}$ and other available information at time t and $N_{\Delta t}$ is the prediction error. Assuming the prediction error is Gaussian distributed, $f(X_{t+\Delta t}^{rx})$ can be expressed as

$$f(X_{t+\Delta t}^{rx}) = \frac{1}{(2\pi)^{3/2}|\Sigma_{\Delta t}|} \exp(-\tilde{X}_{t+\Delta t|t}^{rx\,T} \Sigma_{\Delta t}^{-1} \tilde{X}_{t+\Delta t|t}^{rx}) \quad (3)$$

where $\tilde{X}_{t+\Delta t|t}^{rx} = \hat{X}_{t+\Delta t|t}^{rx} - X_{t+\Delta t}^{rx}$ and $\Sigma_{\Delta t}$ is the covariance matrix of prediction error $N_{\Delta t}$. Let us assume that the variance of the prediction error along each axis changes with the prediction horizon Δt and the non-diagonal elements of $\Sigma_{\Delta t}$ are zero, indicating that prediction errors along each axis are independent. Then, $\Sigma_{\Delta t}$ can be expressed as $\Sigma_{\Delta t} = \sigma_0^2 \Delta t I_3$ where σ_0^2 is the prediction error variance per unit time and I_3 is the 3×3 identity matrix. Based on the estimated location of the UAV-RX with respect to the UAV-TX, the estimated optimal Δt, denoted as $\hat{\Delta t}^*$, to maintain a minimum required beamforming gain $G_{tx,\min}$ can be expressed as

$$\hat{\Delta t}^* = \max_{\Delta t} \quad \Delta t \quad \text{s.t.} \quad \mathbb{E}\{G_{tx}(X_{t+\Delta t}^{rx}, \underline{w}_{t_0})\} \geq G_{tx,\min} \quad (4)$$

where

$$\mathbb{E}\{G_{tx}(X_{t+\Delta t}^{rx}, \underline{w}_{t_0})\} = \int_{\mathbb{D}\{X_{t+\Delta t}^{rx}\}} G_{tx}(X_{t+\Delta t}^{rx}, \underline{w}_{t_0}) f(X_{t+\Delta t}^{rx}) dX_{t+\Delta t}^{rx} \quad (5)$$

and $\mathbb{D}\{X_{t+\Delta t}^{rx}\}$ is the integral domain of $X_{t+\Delta t}^{rx}$. To lower the computational cost of step 2 in Algorithm 1, the numerical

computation of $\mathbb{E}\{G_{tx}(X^{rx}_{t+\Delta t}, \underline{w}_{t_0})\}$ in (5) can be performed using the empirical rule of the Gaussian distribution [14].

We may assume that UAV-RX location $\hat{X}^{rx}_{t|t}$ is measured every ΔT period. Due to processing and measurement delays, $\hat{X}^{rx}_{t|t}$ may be available at the processing unit only after a certain time delay [11]. In addition, there may be a reaction time delay associated with updating $\underline{w}_t$ once the algorithm decides to do so [15]. Let us define the combined processing, measurement and reaction delays as t_d and let the binary variable $D_{w,t} \in \{0, 1\}$ denote the decision of whether or not to update $\underline{w}_t$ at time t.

The Algorithm 1 iteratively updates $\hat{\Delta t}^*$ every ΔT period as it updates $\hat{X}^{rx}_{t|t}$ with new measurements allowing it to adjust $\underline{w}_t$ before G_{tx} reaches $G_{tx,min}$. To avoid the risk of being unable to update $\underline{w}_t$ in a timely manner when $\hat{\Delta t}^* \leq t_d$, the proposed algorithm must make a decision to update $\underline{w}_t$ before $\hat{\Delta t}^*$ falls below t_d. As depicted in Fig. 2, the timeline of the proposed algorithm can be analyzed based on the relative values of t_d and ΔT. The corresponding $\hat{\Delta t}^*$ regions for the first, second, and third scenarios can be written as $\hat{\Delta t}^* > \Delta T + t_d$, $t_d \leq \hat{\Delta t}^* \leq \Delta T + t_d$, and $\hat{\Delta t}^* < t_d$, respectively.

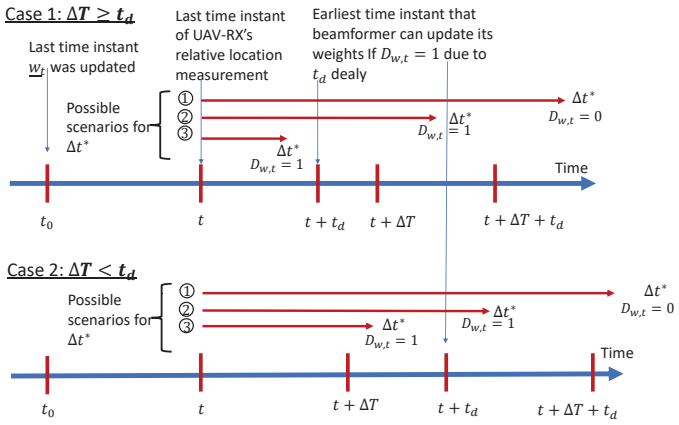

Fig. 2. Timeline of the proposed algorithm

If $\hat{\Delta t}^* > \Delta T + t_d$ in either of the cases depicted in Fig. 2, the algorithm will not update $\underline{w}_t$ (i.e $D_{w,t} = 0$). Instead, it will wait and recalculate $\hat{\Delta t}^*$ with the new observations obtained after ΔT period. On the other hand, whenever $\hat{\Delta t}^* \leq \Delta T + t_d$, the Algorithm makes the decision to update $\underline{w}_t$ at time t ($D_{w,t} = 1$). However, since the change will only take effect at time $t + t_d$, when $\hat{\Delta t}^* < t_d$ in either case, the algorithm will not be able to update $\underline{w}_t$ in a timely manner, causing the beamforming gain G_{tx} to fall below the minimum beamforming gain threshold $G_{tx,min}$. To reduce the occurrence of this scenario and improve the effectiveness of the proposed algorithm in the presence of arbitrary UAV dynamics, an additional gain margin ΔG_d can be incorporated into $G_{tx,min}$ to maintain the desired beamforming gain. With this modification, the $G_{tx,min}$ in (4) can be replaced by $\tilde{G}_{tx,min} = \Delta G_d + G_{tx,min}$ where ΔG_d is an appropriately selected gain margin.

If $t_d \leq \Delta T$ as in Case 1, the proposed Algorithm will be able to adjust the beamforming weights prior to obtaining the subsequent measurement. In this case, the algorithm will iteratively updates $\hat{\Delta t}^*$ every ΔT period as it updates $\hat{X}^{rx}_{t|t}$ with new measurements allowing it to adjust $\underline{w}_t$ before G_{tx} reaches $G_{tx,min}$. It is, however, possible to conceive of a system where $t_d > \Delta T$, although, such a system may not be desired in practice as it is unable to take advantage of faster measurement rates. In this case, the proposed algorithm will need to recalculate $\hat{\Delta t}^*$ after the update of $\underline{w}_t$ (i.e $t_0 \leq t$).

Algorithm 1: Adaptive optimal beamforming weight update period algorithm

Input: $\hat{X}^{rx}_{t|t}$, $\hat{X}^{rx}_{t-\Delta T}$, ...
Output: $D_{w,t}$

Estimate $\hat{X}^{rx}_{t+\Delta t|t}$ for $0 \leq \Delta t \leq \Delta T + t_d$ by using the location prediction method
if $t_0 \leq t$ **then**
  Calculate $\mathbb{E}\{G_{tx}(\underline{w}_{t_0}, X^{rx}_{t+\Delta t|t})\}$ for $0 \leq \Delta t \leq \Delta T + t_d$ based on (3)
  Compute $\hat{\Delta t}^*$ numerically based on (4)
  if $\hat{\Delta t}^* \leq \Delta T + t_d$ **then**
    $D_{w,t} = 1$
    update the beamforming weight to receiver location $\hat{X}^{rx}_{t+t_d|t}$ as $\underline{w}_{t+t_d}$ at $t_0 = t + t_d$
  else
    $D_{w,t} = 0$
else
  $D_{w,t} = 0$
Go back to step 1 with $\hat{X}^{rx}_{t+\Delta T}$

IV. Simulation Results

In this section, we investigate the behaviour of Δt^* with respect to the operating frequency and the effectiveness of the proposed algorithm in the presence of prediction errors.

Recall that $\underline{w}_t$ needs to be updated within Δt^* time to maintain the normalized beamforming gain $G_{tx} \geq G_{tx,\min}$. We assume that the antenna aperture is fixed at $100cm^2$, $G_{tx,\min} = 0.5$ [16], $\frac{d^x}{\lambda} = \frac{d^y}{\lambda} = 0.5$, $r = 30\ m$ and the relative speed of the UAV-RX in the tangential direction with respect to the transmitter UAV is $v_t = 10ms^{-1}$. This corresponds to a relative angular velocity of ω_{rx}= 0.33 rad/s w.r.t. the transmitter. Note that, this particular scenario is assumed only for investigating the relationship between the operating frequency and Δt^*.

The maximum aperture of the transmit antenna can be approximated by the physical area of the antenna, $A_{e,t} = A_{p,t}$ where $A_{p,t}$ denotes the physical area of the transmitter antenna [9]. Since $A_{p,t}$ of the antenna can be expressed as $A_{p,t} = d^x(M^x_{tx} - 1)d^y(M^y_{tx} - 1)$, for a fixed aperture antenna, the number of antenna elements increases as the frequency increases. Hence, for a fixed aperture antenna, the radiation pattern beamwidth becomes narrower as operating frequency

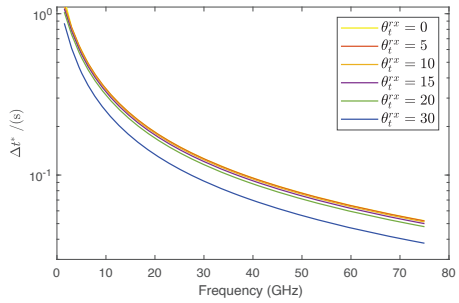

Fig. 3. Dependence of Δt^* on frequency for different initial receiver locations (with transmitter aperture 100 cm^2, $\omega_{rx} = 0.33rad/s$ and $r = 30m$)

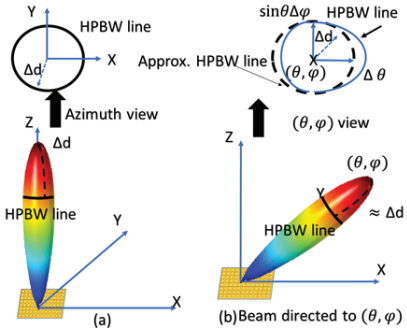

Fig. 4. Comparison transmit signal beam shape when the beam is directed to Z-axis direction and (θ, φ)

increases and, as a result, Δt^* decreases with increasing frequency as shown in Fig. 3.

Figure 3 also shows the variation of Δt^* with the operating frequency when different initial elevation positions are assumed for the UAV-RX. When the signal beam is directed to $(\theta^{rx}, \varphi^{rx})$ position, the shape of the boundary of the HPBW changes with the change in transmit beam direction as shown in Fig. 4. Therefore, Δt^* may vary depending on the position of the UAV-RX at time t according to (1). Figure 3 shows that Δt^* is lower when the transmitter orientation is aligned with the UAV-RX location so that $\theta^{rx} = 0$ than when they are not (i.e $\theta^{rx} \neq 0$).

Smaller Δt^* requires frequent transmission of overhead training bits. Let us consider the same scenario as that in Fig. 3. The overhead bit rate corresponding to Δt^* can be calculated by assuming that the number of overhead bits per beam training process is fixed. Figure 5 shows the dependence of the relative overhead, defined as the ratio between the overhead and total bit rates, on the operating frequency. Clearly, the relative overhead is lower at higher frequencies even with frequent weight updates indicating the advantage of operating in higher frequencies.

To investigate the implications of above findings in a U2U communication system, let us consider a 3D area of $1km \times 1km \times 100m$ [17]. Assume that initially the UAV-TX is located at the center of the cuboidal area and the UAV-RX is placed in a random location within the region. Additionally, it is assumed that both the UAV-RX and UAV-

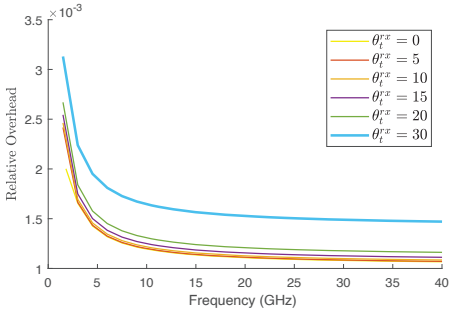

Fig. 5. Variation of the ratio of overhead bitrate and available bitrate with operating frequency

TX move randomly within the specified cuboidal space with speeds ranging from 5 to $15ms^{-1}$ [4]. Every $10ms$, the acceleration of each UAV is randomly set to a value between $-10ms^{-2}$ and $10ms^{-2}$ in each of the three Cartesian axis directions, following a uniform distribution. If any of the UAVs approach the border of the cuboidal area, that particular UAV will accelerate at $5ms^{-2}$ in the opposite direction of the border to avoid crossing it. Note that, the UAV-TX antenna has an aperture of $A_{e,t} = 100cm^2$ and the operating frequency of 60 GHz. Throughout these simulations, we assume that $G_{tx,min} = 0.5$ [16], $\Delta T = 0.1s$ and $t_d = 0.05s$.

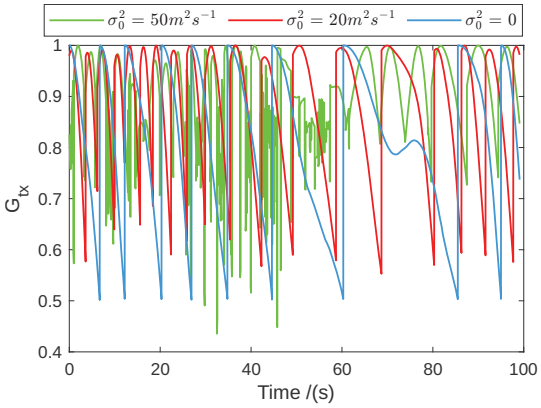

Fig. 6. The variation of beamforming gain G_{tx} of the UAV-RX for different σ_0^2

Figure 6 shows the transmitter beamforming gain as a function of time for different location prediction error variances adopted according to the Algorithm 1. When the flight path prediction is accurate ($\sigma_0^2 = 0$), the proposed algorithm will ensure that G_{tx} does not drop below the required minimum threshold of 0.5 as shown in Fig. 6. However, $\underline{w}_t$ may not always get updated before G_{tx} drops below the threshold when the prediction error variance is non-zero. Occasionally, there is the possibility that G_{tx} may drop below minimum threshold $G_{tx,min}$ due to prediction errors, as can be seen from in Fig. 6 with $\sigma_0^2 = 50m^2s^{-1}$.

Let us denote by P_{out} the probability of G_{tx} dropping below the minimum threshold $G_{tx,min}$ before $\underline{w}_t$ is updated. Figure 7

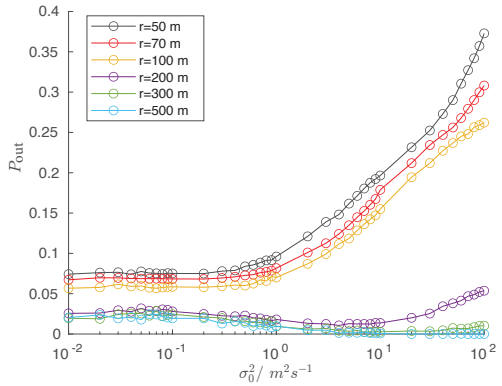

Fig. 7. Dependence of the G_{tx} drops below $G_{tx,min}$ before updating the $\underline{w}_t$ probability P_{out} on the prediction error variance per unit time σ_0^2 when UAV-RX is at a distance of r apart from UAV-TX and $\Delta G_d = 0$

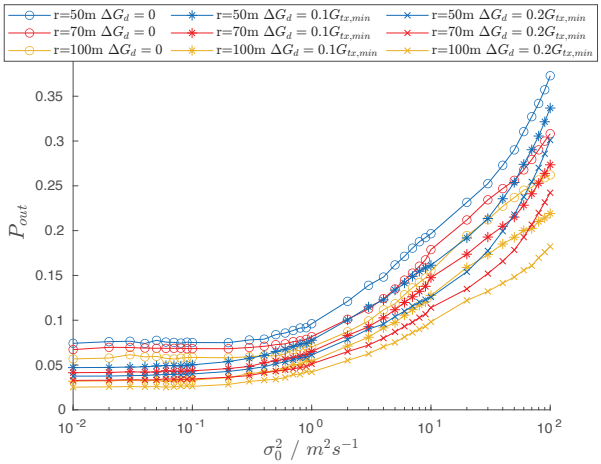

Fig. 8. Dependence of the G_{tx} drops below $G_{tx,min}$ before updating the $\underline{w}_t$ probability P_{out} on the prediction error variance per unit time σ_0^2 when UAV-RX is at a distance of r apart from UAV-TX and different ΔG_d values

demonstrates that once a specific threshold in prediction error variance per second is surpassed, P_{out} increases monotonically with the prediction error variance. Therefore, not surprisingly, the proposed algorithm performs better in systems that have lower estimation error variances. However, when the prediction error is higher, the algorithm may make use of ΔG_d to reduce P_{out}. By utilizing different ΔG_d values, Fig. 8 shows the improved P_{out} performance by 10-20%. Depending on the required P_{out}, distance between UAVs and the prediction error variance, ΔG_d value can be selected. Therefore, by using the proposed algorithm, stable connection between UAV-BS and UAV-UE can be maintained accurately even with the presence of prediction error.

V. Conclusion

The paper investigated the optimal update timing for the transmit beamformer weights in order to maintain a stable connection between two UAVs. The study found that in order to calculate optimal Δt, it was necessary to have knowledge of the flight path of the UAV-RX relative to the UAV-TX. It was also observed that as the operating frequency increased, the relative overhead decreased indicating that even with more frequent weight updates, using mmWave frequencies can lead to better throughput performance.

The proposed algorithm for determining the beamformer weight update timing was tested in a U2U communication system. The results showed that when accurate UAV-RX location prediction was available the beamforming gain remained consistently above the minimum threshold resulting in a stable connection. As expected, when there is a non-zero location prediction error, there is a corresponding non-zero probability of beamformer gain falling below the desired threshold which increases with the variance of the prediction error. However, we also observe that incorporating a gain margin ΔG_d helps reduce this by 10-20% resulting in more stable connections between UAVs in the presence of non-zero location prediction errors.

References

[1] K. Prabhath, S. K. Jayaweera, and S. A. Lane, "Intelligent reflecting surface orientation optimization to enhance the performance of wireless communications systems," in *The 17th Int. Workshop Antenna Technol. (iWAT)*, Dublin, Ireland, May 2022, pp. 65–68.

[2] G. Militaru, D. Popescu, and L. Ichim, "UAV-to-UAV communication options for civilian applications," in *2018 26th Telecommun. Forum (TELFOR)*, Belgrade, Serbia, Nov. 2018, pp. 1–4.

[3] S. Zhang *et al.*, "Cellular UAV-to-X communications: Design and optimization for multi-UAV networks," *IEEE Trans. Wirel. Commun.*, vol. 18, no. 2, pp. 1346–1359, Feb 2019.

[4] Y. Zeng, Q. Wu, and R. Zhang, "Accessing from the sky: A tutorial on UAV communications for 5G and beyond," *Proc. IEEE*, vol. 107, no. 12, pp. 2327–2375, Dec 2019.

[5] P. S. Bithas *et al.*, "UAV-to-ground communications: Channel modeling and UAV selection," *IEEE Trans. Wirel. Commun.*, vol. 68, no. 8, pp. 5135–5144, Aug 2020.

[6] L. Zhu *et al.*, "3-D beamforming for flexible coverage in millimeter-wave UAV communications," *IEEE Wirel. Commun.*, vol. 8, no. 3, pp. 837–840, June 2019.

[7] H.-L. Song and Y.-C. Ko, "Robust and low complexity beam tracking with monopulse signal for UAV communications," *IEEE Trans. Veh. Technol.*, vol. 70, no. 4, pp. 3505–3513, April 2021.

[8] W. Tang *et al.*, "Wireless communications with reconfigurable intelligent surface: Path loss modeling and experimental measurement," *IEEE Trans. Wirel. Commun.*, vol. 20, no. 1, p. 421–439, Jan 2021.

[9] C. A. Balanis, *Antenna Theory: Analysis and Design*, 2nd ed. John Wiley Sons, 1997.

[10] B. Ning *et al.*, "A unified 3D beam training and tracking procedure for terahertz communication," *IEEE Trans. Wirel. Commun.*, vol. 21, no. 4, pp. 2445–2461, 2022.

[11] S. Wang, A. Then, and R. Herschel, "UAV tracking based on unscented kalman filter for sense and avoid applications," in *2020 21st Intl. Radar Symposium (IRS)*, 2020, pp. 250–255.

[12] X. Liu *et al.*, "Machine learning aided trajectory design and power control of multi-UAV," in *2019 IEEE Global Communications Conference (GLOBECOM)*, 2019, pp. 1–6.

[13] P. Shu *et al.*, "Trajectory prediction of UAV based on LSTM," in *2021 2nd Intl. Conference on Big Data & Artificial Intelligence & Software Engineering (ICBASE)*, 2021, pp. 448–451.

[14] S. Tsumoto, "Empirical rule induction methods selection," in *2021 IEEE International Conference on Big Data (Big Data)*, 2021, pp. 5561–5570.

[15] M. N. Hamdy, "Beamformers explained," in *Commscope*, 2019, pp. 1–6.

[16] A. Simonsson *et al.*, "Beamforming gain measured on a 5G test-bed," in *IEEE 85th Veh. Technol. Conf. (VTC) Spring*, Sydney, NSW, Australia, June 2017, pp. 1–5.

[17] A. B. Bhandarkar and S. K. Jayaweera, "Optimal trajectory learning for UAV-mounted mobile base stations using RL and greedy algorithms," in *17th Int. Conf. Wirel. Mob. Comput. Netw. Commun. (WiMob)*, Bologna, Italy, Oct 2021, pp. 13–18.